J|A|C|S ARTICLES

Published on Web 04/10/2009

Multiple H-Bonds Directed Self-Assembly of an Amphiphilic and Plate-Like Codendrimer with Janus Faces at Water−Air Interface

Miao Yang,[†] Wei Wang,[†,*] Ingo Lieberwirth,[‡] and Gerhard Wegner[‡,*]

The Key Laboratory of Functional Polymer Materials of Ministry of Education and Institute of Polymer Chemistry, College of Chemistry, Nankai University, Tianjin 300071, China, and Max-Planck-Institute for Polymer Research, Ackermannweg 10, Postfach 3148, D-55128, Mainz, Germany

Received February 5, 2009; E-mail: weiwang@nankai.edu.cn; wegner@mpip-mainz.mpg.de

Abstract: An amphiphilic diblock codendrimer composed of a third generation poly(methallyl dichloride) end-capped by eight hydroxyl groups (PMDC$(OH)_8$) and a second generation poly(urethane amide) end-capped by four alkyl groups (PUA$(C16)_4$) were found to self-assemble into highly oriented ribbons at the water−air interface. Further investigation on the ribbon formation shows that the ribbons are hierarchically self-organized by the janus and plate-like shape of g3-PMDC$(OH)_8$-*b*-g2-PUA$(C16)_4$. Sextuple H-bonds existing at different positions of the molecular plate are the main driving force for the one-dimensional growth of the ribbon. The recognition of these H-bonds leads to a highly ordered stacking of the codendrimers, and the crystallization of the alkyl chains results in a primary ribbon with a *ca.* 7.6 ± 0.5 nm width. The primary ribbons prefer to organize into secondary ribbons with an average width of 53 ± 6.0 nm. The manner of recognition and assembly is similar to the organization of a kind of toy building block with janus faces, which provides a new strategy to the design of well-defined nanomaterials.

Introduction

Over the past 30 years supramolecular self-assembly has attracted great attention not only because a huge amount of artificial assemblies were created for numerous purposes by this method[1−8] but also because it is an intriguing process in natural living systems such as in the formation of the double-helical structure of DNA[9] and the α-helix (or β-sheet) conformation of natural proteins.[10−12] The main driving force for molecular self-assembly is always noncovalent bonds, among which the hydrogen bond plays an important role in directing spontaneous organization into complex structures.[13−20] Hydrogen bonds (H-bond) are directional and of moderate intensity.[21] This provides us an opportunity to build up versatile arrays of H-bonding donor (D) and acceptor (A) sites. The planar arrays of D and A sites, such as a centrosymmetric AD-DA array,[22] triple H-bonding motifs,[13,23−26] quadruple H-bonding motifs,[15,27] and so on,[28,29] have been extensively investigated in the past decades. Intermolecular H-bonds have also been explored to direct the low molecular weight gelators to form a series of hierarchical assemblies such as nanofibers, nanotubes, and nanocrystals.[30−42]

[†] Nankai University.
[‡] Max-Planck-Institute for Polymer Research.

(1) Lehn, J.-M. *Angew. Chem., Int. Ed.* **1988**, *27*, 89–112.
(2) Brunsveld, L.; Folmer, B. J. B.; Meijer, E. W.; Sijbesma, R. P. *Chem. Rev.* **2001**, *101*, 4071–4097.
(3) Moore, J. S. *Curr. Opin. Colloid Interface Sci.* **1999**, *4*, 108–116.
(4) Lehn, J.-M. *Supramolecular Chemistry: Concepts and Perspectives*; Wiley-VCH: Weinheim, 1995.
(5) Greef, T. F. A.; Meijer, E. W. *Nature (London)* **2008**, *453*, 171–173.
(6) Lawrence, D. S.; Jiang, T.; Levett, M. *Chem. Rev.* **1995**, *95*, 2229–2260.
(7) Shimizu, T.; Masuda, M.; Minamikawa, H. *Chem. Rev.* **2005**, *105*, 1401–1444.
(8) Desiraju, G. R. *Nature (London)* **2001**, *412*, 397–400.
(9) Saenger, W. *Principles of Nucleic Acid Structure*; Springer: Berlin, 1984.
(10) Pauling, L.; Corey, R. B. *Proc. Natl. Acad. Sci. U.S.A.* **1951**, *37*, 235–240.
(11) Pauling, L.; Corey, R. B. *Proc. Natl. Acad. Sci. U.S.A.* **1951**, *37*, 241–250.
(12) Pauling, L.; Corey, R. B. *Proc. Natl. Acad. Sci. U.S.A.* **1951**, *37*, 251–256.
(13) Prins, L. J.; Reinhoudt, D. N.; Timmerman, P. *Angew. Chem., Int. Ed.* **2001**, *40*, 2383–2426.
(14) Clark, T. D.; Ghadiri, M. R *J. Am. Chem. Soc.* **1995**, *117*, 12364–12365.
(15) Schmuck, C.; Wienand, W. *Angew. Chem., Int. Ed.* **2001**, *40*, 4363–4369.
(16) Sherrington, D. C.; Taskinen, K. A. *Chem. Soc. Rev.* **2001**, *30*, 83–93.
(17) Rehm, T.; Schmuck, C. *Chem. Commun.* **2008**, 801–813.
(18) Bushey, M. L.; Hwang, A.; Stephens, P. W.; Nuckolls, C. *Angew. Chem., Int. Ed.* **2002**, *41*, 2828.
(19) Bushey, M. L.; Nguyen, T. Q.; Zhang, W.; Horoszewski, D.; Nuckolls, C. *Angew. Chem., Int. Ed.* **2004**, *43*, 5446–5453.
(20) Ghadiri, M. R.; Granja, J. R.; Milligan, R. A.; McRee, D. E.; Khazanovich, N. *Nature (London)* **1993**, *366*, 324–327.
(21) Jeffrey, G. A. *An Introduction to Hydrogen Bonding*; Oxford University Press: Oxford, 1997.
(22) Griessl, S.; Lackinger, M.; Edelwirth, M.; Hietschold, M.; Heckl, W. M. *Single Molecules* **2002**, *3*, 25–31.
(23) Marsh, A.; Silvestri, M.; Lehn, J. M. *Chem. Commun.* **1996**, 1527–1528.
(24) Whitesides, G. M.; Simanek, E. E.; Mathias, J. P.; Seto, C. T.; Chin, D.; Mammen, M.; Gordon, D. M. *Acc. Chem. Res.* **1995**, *28*, 37–44.
(25) Zimmermann, S. C.; Corbin, P. S. *Struct. Bonding (Berlin)* **2000**, 63–94.
(26) Beijer, F. H.; Sijbesma, R. P.; Vekemans, J. A. J. M.; Meijer, E. W.; Kooijman, H.; Spek, A. L. *J. Org. Chem.* **1996**, *61*, 6371–6380.
(27) Sijbesma, R. P.; Meijer, E. W. *Chem. Commun.* **2003**, 5–16.
(28) Zeng, H.; Ickes, H.; Flowers, R. A.; Gong, B. *J. Org. Chem.* **2001**, *66*, 3574–3583.
(29) Corbin, P. S.; Zimmerman, S. C. *J. Am. Chem. Soc.* **2000**, *122*, 3779–3780.

Dendrimer-based molecules (or macromolecules) are one of the most promising candidates in constructing assemblies owing to their well-defined architectures and diversity in functionalization.[43−46] A series of classic works have shown the perfect organization of different dendrons into supramolecular spheres or cylinders due to their specific molecular shape.[47−50] Multiple intermolecular H-bonding from amide (or urethane) groups in bola-form dendritic molecules[51−56] and dendrons[57−60] plays a key role in constituting one-dimensional (1D) assemblies that further built up supramolecular networks in gels. Uniform ribbon-like aggregates were formed from dendritic rod−coil molecules because of the accurate matching of carboxyl groups in the rod dendrons through H-bonds.[61,62] These studies show that a well-defined molecular shape, intermolecular driving forces, and molecular rigidity are important factors for the formation of 1D aggregates. Though dendritic molecules with specified shapes show innate advantages in acting as building blocks, it is still challenging to design molecules with accurately matched functional groups between molecules for the purpose of maximum efficiency of driving forces in assembling.

In our group a class of diblock codendrimers, which are composed of two unlike dendrons covalently linked in their focal point, has been developed and their self-assemblies have been studied in the past years.[63−66] In comparison with parent dendrons, the molecular shape of codendrimers can be adjusted in a wide range by simply changing the dendron generation and different functional groups can be precisely placed at the branched units and peripheries of two dendrons; therefore, their assembly capability can be tuned in a wide range. Our previous findings have demonstrated that these codendrimers can self-organize into vesicles with different topologies in selective solvents,[63,64] 1D nanoribbons in organic gels,[65] and a layered structure in bulk phase.[66] These works introduced a concept that diblock codendrimers can self-organize into supramolecular assemblies with versatile morphologies closely associated with the specific molecular shape and multiple intermolecular interactions. In the present study, we put further efforts in understanding a highly efficient organization of nanoribbons of a plate-like, amphiphilic codendrimer at the water−air interface. The codendrimer used is composed of third generation poly(methallyl dichloride) ($PMDC(OH)_8$) end-capped by eight hydroxyl groups and second generation poly(urethane amide) end-capped four alkyl groups ($PUA(C16)_4$). The codendrimer is denoted as g3-$PMDC(OH)_8$-*b*-g2-$PUA(C16)_4$, and its chemical structure is shown in Scheme 1A. The eight hydroxyl groups on the periphery of the PMDC block and the four alkyl groups on the periphery of the PUA block endow the amphiphility to the compound. Consequently, it assembles at the water−air interface to form a monolayer. Most importantly, there are two amides and four urethane residues in the body of the codendrimer, which can provide multiple H-bonding between molecules. In this study we will show that because of the specific chemical structure of this codendrimer it displays a plate-like shape of which one face has six N−H groups (or H-bond donors) and another face has six C═O groups (or H-bond acceptors) in the self-assembled structure. The toys in Scheme 1B vividly depict the janus feature of the codendrimers and their face-to-face recognition and assembly. Because such a janus face feature can bring a maximum number of intermolecular N−H...O═C bonds, the donor face of a molecule can spontaneously recognize the acceptor face of another molecule. Such a molecular recognition means a full match of the six H-bond sites to further generate the maximum driving force for their assembly in the form of ordered supramolecular objects. Our investigation illustrates that the face-to-face recognition of the plate-like codendrimer in the molecular self-assembly follows

(30) Coe, S.; Kane, J. J.; Nguyen, T. L.; Toledo, L. M.; Wininger, E.; Fowler, F. W.; Lauher, J. W. *J. Am. Chem. Soc.* **1997**, *119*, 86–93.
(31) John, G.; Masuda, M.; Okada, Y.; Yase, K.; Shimizu, T. *Adv. Mater.* **2001**, *13*, 715–718.
(32) Zimmerman, S. C.; Zeng, F.; Reichert, D. E. C.; Kolotuchin, S. V. *Science* **1996**, *271*, 1095–1098.
(33) Philp, D.; Stoddart, J. F. *Angew. Chem., Int. Ed.* **1996**, *35*, 1154–1196.
(34) Whitesides, G. M.; Mathias, J. P.; Seto, C. T. *Science* **1991**, *254*, 1312–1319.
(35) Storhoff, J. J.; Mirkin, C. A. *Chem. Rev.* **1999**, *99*, 1849–1862.
(36) Shimizu, T.; Masuda, M. *J. Am. Chem. Soc.* **1997**, *119*, 2812–2818.
(37) Shimizu, T.; Ohnishi, S.; Kogiso, M. *Angew. Chem., Int. Ed.* **1998**, *37*, 3260–3262.
(38) Shimizu, T.; Iwaura, R.; Masuda, M.; Hanada, T.; Yase, K. *J. Am. Chem. Soc.* **2001**, *123*, 5947–5955.
(39) Shimizu, T.; Kogiso, M.; Masuda, M. *J. Am. Chem. Soc.* **1997**, *119*, 6209–6210.
(40) Jung, J. H.; Kobayashi, H.; Masuda, M.; Shimizu, T.; Shinkai, S. *J. Am. Chem. Soc.* **2001**, *123*, 8785–8789.
(41) Masuda, M.; Hanada, T.; Okada, Y.; Yase, K.; Shimizu, T. *Macromolecules* **2000**, *33*, 9233–9238.
(42) Frankel, D. A.; O'Brien, D. F. *J. Am. Chem. Soc.* **1994**, *116*, 10057–10069.
(43) Emrick, T.; Fréchet, J. M. J. *Curr. Opin. Colloid Interface Sci.* **1999**, *4*, 15–23.
(44) Smith, D. K.; Hirst, A. R.; Love, C. S.; Hardy, J. G.; Brignell, S. V.; Huang, B. Q. *Prog. Polym. Sci.* **2005**, *30*, 220–293.
(45) Zeng, F. W.; Zimmerman, S. C. *Chem. Rev.* **1997**, *97*, 1681–1712.
(46) Newkome, G. R.; He, E. F.; Moorefield, C. N. *Chem. Rev.* **1999**, *99*, 1689–1746.
(47) Percec, V.; Ahn, C. H.; Ungar, G.; Yeardley, D. J. P.; Möller, M.; Sheiko, S. S. *Nature (London)* **1998**, *391*, 161–164.
(48) Hudson, S. D.; Jung, H. T.; Percec, V.; Cho, W. D.; Johansson, G.; Ungar, G.; Balagurusamy, V. S. K. *Science* **1997**, *278*, 449–452.
(49) Balagurusamy, V. S. K.; Ungar, G.; Percec, V.; Johansson, G. *J. Am. Chem. Soc.* **1997**, *119*, 1539–1555.
(50) Percec, V.; Cho, W. D.; Mosier, P. E.; Ungar, G.; Yeardley, D. J. P. *J. Am. Chem. Soc.* **1998**, *120*, 11061–11070.
(51) Newkome, G. R.; Baker, G. R.; Saunders, M. J.; Russo, P. S.; Gupta, V. K.; Yao, Z. Q.; Miller, J. E.; Bouillion, K. *J. Chem. Soc., Chem. Commun.* **1986**, 752–753.
(52) Newkome, G. R.; Moorefield, C. N.; Baker, G. R.; Beheru, R. K.; Escamillia, G. H.; Saunders, M. J. *Angew. Chem., Int. Ed.* **1992**, *31*, 917–919.
(53) Newkome, G. R.; Baker, G. R.; Arai, S.; Saunders, M. J.; Russo, P. S.; Theriot, K. J.; Moorefield, C. N.; Rogers, L. E.; Miller, J. E. *J. Am. Chem. Soc.* **1990**, *112*, 8458–8465.
(54) Huang, B. Q.; Hirst, A. R.; Smith, D. K.; Castelletto, V.; Hamley, I. W. *J. Am. Chem. Soc.* **2005**, *127*, 7130–7139.
(55) Hirst, A. R.; Smith, D. K.; Feiters, M. C.; Geurts, H. P. M.; Wright, A. C. *J. Am. Chem. Soc.* **2003**, *125*, 9010–9011.
(56) Partridge, K. S.; Smith, D. K.; Dykes, G. M.; McGrail, P. T. *Chem. Commun.* **2001**, 319–320.
(57) Jang, W.-D.; Jiang, D.-L.; Aida, T. *J. Am. Chem. Soc.* **2000**, *122*, 3232–3233.
(58) Kim, C.; Kim, K. T.; Chang, Y.; Song, H. H.; Cho, T.-Y.; Jeon, H.-J. *J. Am. Chem. Soc.* **2001**, *123*, 5586–5587.
(59) Jang, W. D.; Aida, T. *Macromolecules* **2003**, *36*, 8461–8469.
(60) Ji, Y.; Luo, Y.-F.; Jia, X.-R.; Chen, E.-Q.; Huang, Y.; Ye, C.; Wang, B.-B.; Zhou, Q.-F.; Wei, Y. *Angew. Chem., Int. Ed.* **2005**, *44*, 6025–6029.
(61) Zubarev, E. R.; Pralle, M. U.; Sone, E. D.; Stupp, S. I. *J. Am. Chem. Soc.* **2001**, *123*, 4105–4106.
(62) Zubarev, E. R.; Sone, E. D.; Stupp, S. I. *Chem.−Eur. J.* **2006**, *12*, 7313–7327.
(63) Yang, M.; Wang, W.; Yuan, F.; Zhang, X. W.; Li, J. Y.; Liang, F. X.; He, B. L.; Minch, B.; Wegner, G. *J. Am. Chem. Soc.* **2005**, *127*, 15107–15111.
(64) Yuan, F.; Zhang, X. J.; Yang, M.; Wang, W.; Minch, B.; Lieser, G.; Wegner, G. *Soft Matter* **2007**, *3*, 1372–1376.
(65) Yang, M.; Zhang, Z.; Yuan, F.; Wang, W.; Hess, S.; Lienkamp, K.; Lieberwirth, I.; Wegner, G. *Chem.−Eur. J.* **2008**, *14*, 3330–3337.
(66) Yuan, F.; Wang, W.; Yang, M.; Zhang, X. J.; Li, J. Y.; Li, H.; He, B. L. *Macromolecules* **2006**, *39*, 3982–3985.

Scheme 1. (A) Structural Feature of g3-PMDC(OH)$_8$-*b*-g2-PUA(C16)$_4$ and (B) a Photo Showing Assembly of Two Pieces of Toy with a Janus Face

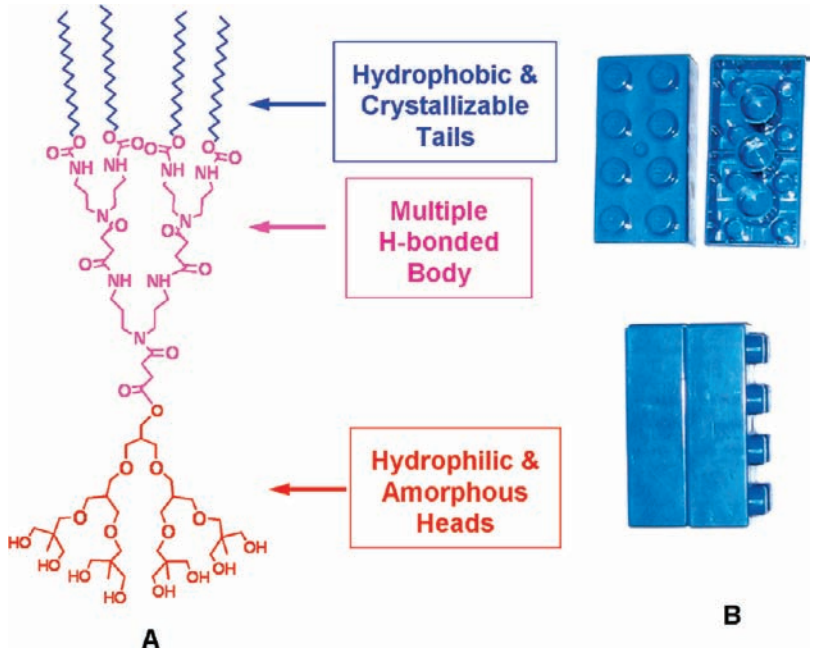

a process and exhibits a mechanism different from conventional surfactants or amphiphilic copolymers forming single molecular layers.

Results and Discussion

Synthesis and Structural Feature of the Codendrimer. The synthesis of the codendrimer g3-PMDC(OH)$_8$-*b*-g2-PUA(C16)$_4$ has been developed in our group and can be found in the Supporting Information.[65] The purity and the structural identity of this molecule were assessed by a combination of ^{1}H NMR and ^{13}C NMR spectroscopy, MALDI-TOF mass spectrometry, and elemental analysis. Scheme 1A shows the chemical structure of this molecule and the functional features of the different groups. On the periphery of the PUA block there are four hydrophobic hexadecyl tails, and in the body of the PUA block there are two amide and four urethane groups providing six potential sites for intermolecular H-bonding. On the periphery of the PMDC block, there are eight hydroxyl groups acting as hydrophilic heads. Compared to traditional surfactants or amphiphilic copolymers, the plate-like shape of this codendrimer in combination with an amphiphilic feature and multiple intermolecular interactions in the janus faces will be the key factors of controlling the manner of molecular organization. In other words, the key factor, which this study focuses on, is to understand the face-to-face recognition in the self-assembly of the codendrimer.

Formation and Morphology of Ribbons at Water−Air Interface. The amphiphilic codendrimer forms monolayer aggregates at the water−air interface. When its solution in chloroform (1 g/L, 30 μL) was gently dropped onto a water surface (mili-Q, water−air interface area: 20 cm^2), the amphiphilic molecules quickly spread on the water surface. A piece of silica wafer was immerged into the solution and slowly lifted up. Small pieces of membranes were observed on the silica wafer by scanning electron microscopy (SEM) as shown in Figure 1A. These membranes have a uniform thickness, indicating that they consist of a monolayer. A high magnification SEM micrograph in Figure 1B shows that these membranes display a flag-like shape: The triangle-shape membranes are "flags", and long and thin ribbons are "flagpoles". Usually, the edges containing the flagpole are sharp and straight. Three days later, in our SEM observation we found that the flag-like membranes had completely disappeared, thus only ribbons at nanoscale with a narrow width distribution were observed in the same solution as shown in Figure 1C. This indicates that a morphological change occurred in the system before transferring to the surface of silicon wafer. Because of the very thin width of the ribbons, it is difficult to make an in situ observation directly at the water−air interface. It may be argued that the observed morphologies are not a full representation of those at the water−air interface. In fact the method of transferring monolayers from water surface to the surface of solid substrates is frequently used in Langmuir−Blodgett film preparation. It is commonly accepted that the transformation will be not able to change any morphology formed at the water−air interface. The morphology of the final ribbon did not change with time (at least three months). It means that they are at least metastable under given conditions. Interestingly, the width of the final ribbon corresponds to the width of the ribbon growing along the membrane at the beginning. Therefore, it is reasonable to believe that the ribbons have detached themselves from the original membranes.

Transmission electron microscopy (TEM) investigation on the self-assembled ribbons shows that on the water surface these ribbons build up an ordered pattern similar to that of rodlike molecules in their liquid crystal phase. The image in Figure 2A clearly displays a disclination of strength $s = +1/2$. The zoom-in image in Figure 2B shows that the ribbons are always straight without bending; thus the long ribbons can occasionally break into two pieces to fit the curvature as indicated by red arrows. Accordingly, these ribbons appear to be highly rigid, an indication of a well-defined crystalline packing of the molecules. Figure 3 shows the width and length distributions of the ribbons, respectively, obtained from 285 ribbons. The width distribution fits a Gaussian curve with an average width of 53 ± 6.0 nm. The length distribution of the ribbon seems

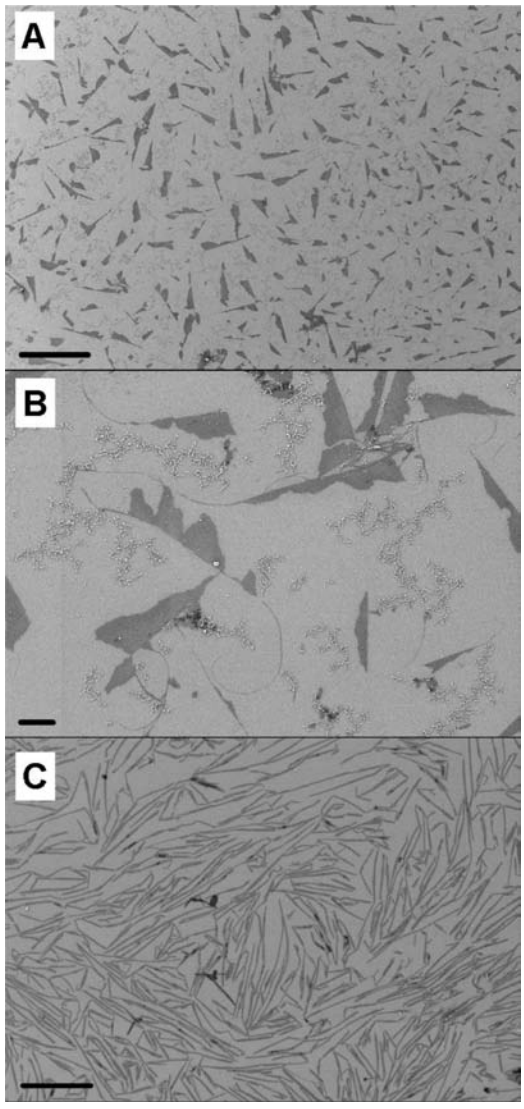

Figure 1. SEM images showing the aggregates of g3-PMDC(OH)$_8$-*b*-g2-PUA(C16)$_4$ formed at the water−air interface. (A) The image was obtained at *ca.* 0 h, and the scale bar is 10 μm. (B) The zoom-in image of image A. The scale bar is 1 μm. (C) The image was obtained after 3 days. The scale bar is 2 μm.

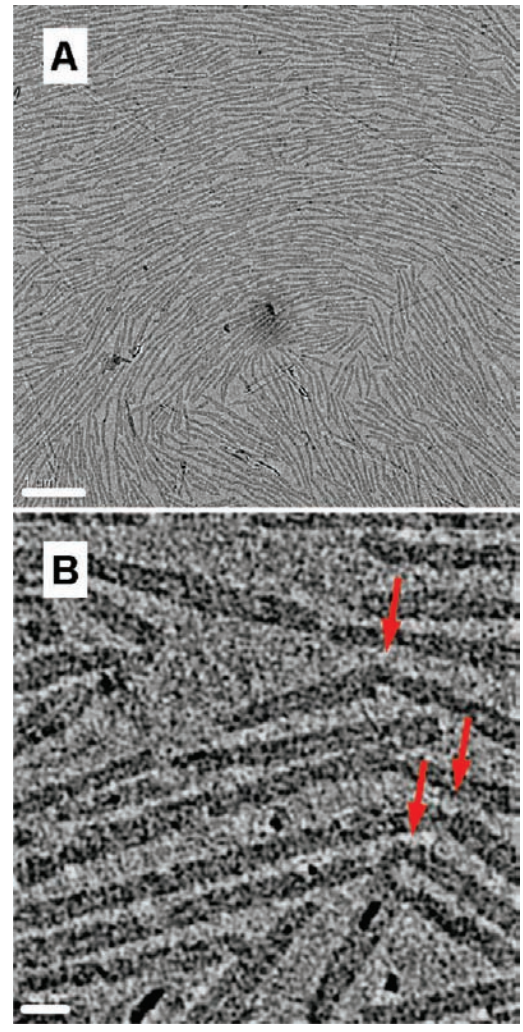

Figure 2. (A) TEM image showing an ordered pattern formed by the ribbons at the water−air interface. There is a disclination of a strength $s = +1/2$. The scale bar is 1 μm. (B) This is an enlarged TEM image showing several breakages of the ribbons, as pointed by the arrows, to fit the curvature. The scale bar is 100 nm.

random. The typical length of the ribbon is in the range from 400 nm to 2 μm. Ribbons longer than 2 μm are quite rare, probably because of their brittleness when exposed to mechanical stress.

Because of the weak contrast, high magnification TEM images can not give further evidence for the internal and fine structure within the ribbons. But, fortunately, the characterization using atomic force microscopy (AFM) gave explicit information about the fine morphology within the ribbons. The AFM image in Figure 4A clearly shows that the ribbons are composed of several fine ribbons. In Figure 4B the height profile across the width direction shows a *ca.* 2.8 nm thickness of the ribbons that indicates that they consist of a monolayer. Therefore, it is reasonable to imagine that due to the amphiphilic feature the codendrimer should stand on the water surface. It is necessary to distinguish the two kinds of ribbons found in this study. Here we define the fine ribbon as the primary ribbon and the ribbon composed of the primary ribbons as the secondary ribbon. The direct measurement by AFM shows that the primary ribbon is *ca.* 20 nm wide. However, it is worth noting that when a sample is on the same size scale as the AFM tip, the convolution effect can broaden the observed size of the sample. So, the value of 20 nm is not the real width of the primary ribbons. From a large number of measurements we found that the number of primary ribbons packing in an individual secondary ribbon is variable. We measured the width of the secondary ribbon and the number N of the primary ribbons within the secondary ribbons from the AFM images. Figure 5 shows a linear plot of this width versus N. The slope gives the average width of the primary ribbon as 7.6 $\pm$ 0.5 nm. This is a value obtained under the condition of avoiding the convolution effect. Driven by H-bonds the molecules first self-organized into the primary ribbons with a *ca.* 7.6 nm width. Afterward, the primary ribbons arrange parallel to form the secondary ribbons with a *ca.* 53 nm width on average. This width value indicates that the secondary ribbon consists of seven primary ribbons on average. The whole process is a typical hierarchical organization of the codendrimer that we will discuss in more detail in the following subsection.

Internal Structure of Primary Ribbon. At the water−air interface the ribbons were found to form an ordered pattern because of the high rigidity. The oriented ribbons in a large

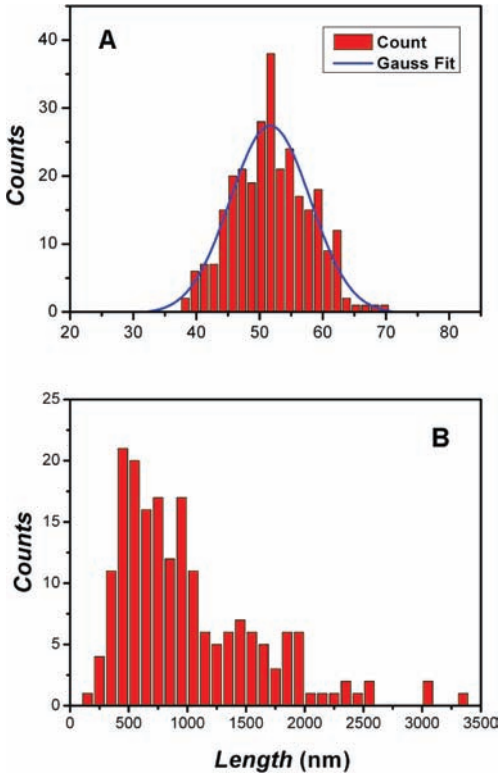

Figure 3. Size distribution of the width (A) and length (B) of the ribbons observed by TEM.

area help to obtain an electron diffraction (ED) pattern that could be used to investigate the internal structure of the ribbon. Figure 6 shows the ribbons oriented along the direction as indicated by the arrow, and the inset shows the ED pattern obtained from an area with a diameter of ~200 nm in which there are only a couple of similar oriented ribbons. So, this ED pattern is similar to a fiber texture diffraction of single crystals. The 10 diffraction dots clearly indicate the crystalline ribbon has a highly ordered structure. To evaluate the exact distance of the diffractions in the ED pattern, a wide-angle X-ray powder diffractogram was obtained, as shown in Figure 7. There are three peaks appearing at d values of 4.60, 3.90, and 3.67 Å. These three peaks correspond to the diffraction spots in the ED pattern. We denote the different diffraction spots using different colors as shown in Figure 8. These diffraction spots have their origin in the sublattice in the alkyl chains. Four blue diffraction spots have a d value of 4.60 Å, two red diffraction spots have a d value of 3.90 Å, and four green diffraction spots have a d value of 3.67 Å, respectively. These diffractions are contributed by the crystallized alkyl chains in the codendrimer. At first glance, this diffraction pattern is different from those of simple alkanes or polyethylene single crystals. To understand the pattern we tried to divide the original diffractions into two groups of diffractions as shown in Figure 8. Further, we performed a computer simulation[67] on the crystal with the alkyl chains packed in a monoclinic lattice. The experimental diffraction and calculated diffraction fit very well, as shown in Figure 9A and B. The data of the diffractions are listed in Table 1. The unit cell constants of the crystal are as follows: $a = 4.19$ Å, $b = 4.95$ Å, and $c =$ --; $\alpha = 90°$, $\beta = 90°$, and $\gamma = 111.5°$.[68,69] Figure 9C shows the corresponding packing of the alkyl chains in the crystal of four molecules. These results show that the ribbon grows along the b axis. Because of the amphiphilic structure the hydroxyl groups in the PMDC block should directly contact the water and the alkyl chains in the periphery of the PUA block are directed to the air. It means that the chains are forced to

(67) Cerius 2 software is used to simulate the ED pattern using polyethylene as the model.

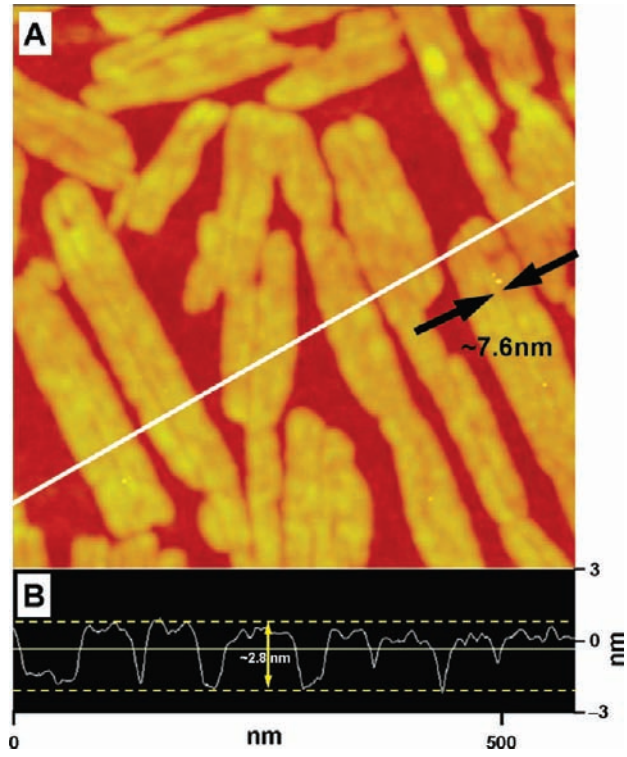

Figure 4. (A) Height AFM image, obtained in tapping mode, showing ribbons on the surface of silica wafer. The finer primary ribbons with a *ca.* 7.6 nm width can be seen in this image. The scan size is 500 nm × 500 nm, and the z scale is 10 nm. (B) Height profile across the width direction showing a *ca.* 2.8 nm thickness of the ribbons.

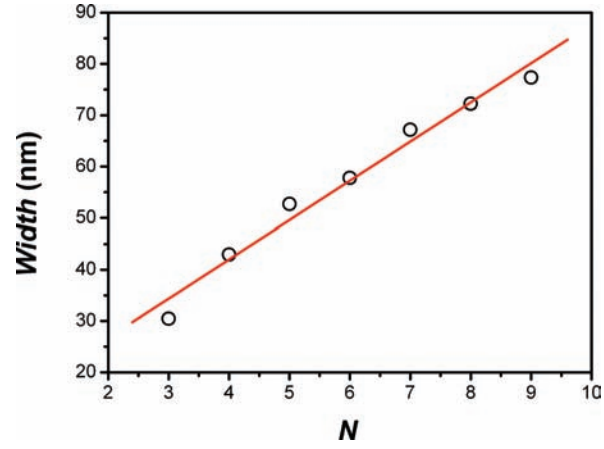

Figure 5. Plot of the total width of the secondary ribbons versus the number, N, of primary ribbons in a secondary ribbon. The slope gives the 7.6 nm width of the primary ribbon.

(68) Since the c axis is parallel to the incident electron beam, it is impossible to obtain its value. For a monolayer of surfactant containing alkyl chains, $c \approx 2.54$ Å when the hydrocarbon chain takes the form of a zigzag from literature.[69]

(69) Petty, M. C. *Langmuir-Blodgett Films: An introduction*; Cambridge University Press: Cambridge, 1996.

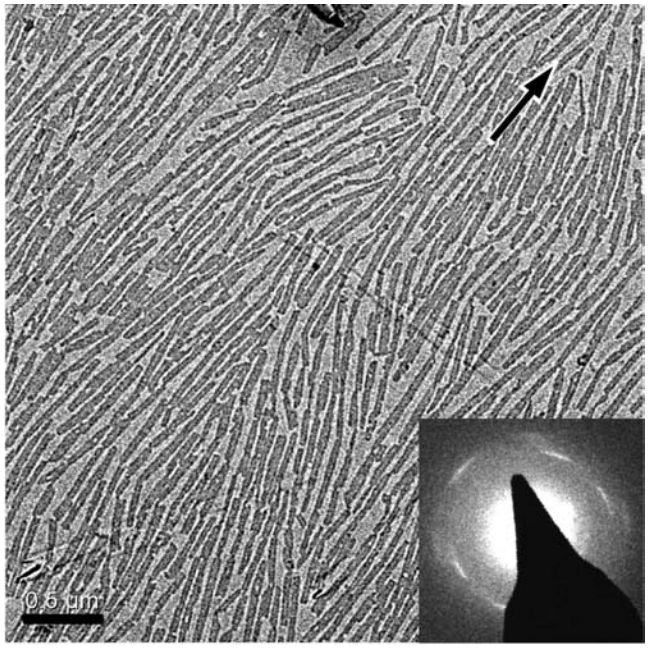

Figure 6. TEM image of the oriented ribbons and ED pattern obtained for a few oriented ribbons. This ED pattern clearly shows that the ribbon is high crystallized. The scale bar is 500 nm.

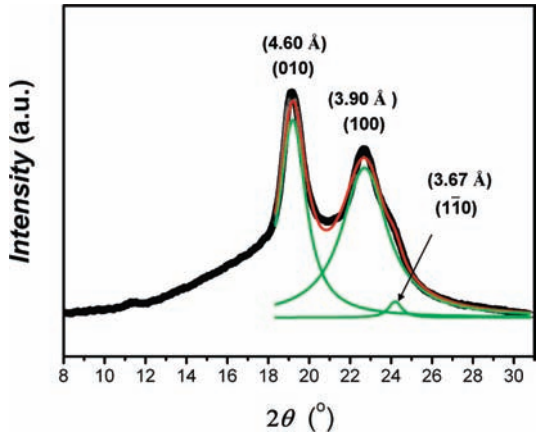

Figure 7. Wide-angle X-ray powder diffractogram of the alkyl chain crystal in the ribbons of g3-PMDC$(OH)_8$-*b*-g2-PUA$(C16)_4$. The *d*-spacings and Miller index are indicted.

stay perpendicular to the water surface. Therefore, the alkyl chains crystallize in the supramolecular ribbon.

Formation of Multiple H-Bonds in Primary Ribbons. Because of the specific chemical structure of this codendrimer, multiple H-bonds were considered as the main driving force for the molecular self-assembly. The four urethane groups are directly connected to the alkyl chains; thus H-bonds between them play a key role in controlling the ribbon-like crystal of the alkyl chains. Infrared (IR) analysis shows that the band of C−N stretching appears at 1278 cm^{-1} (see Figure S2), indicating that the urethane groups take a *trans*-orientation in the crystal. This further means that the urethane groups were connected by H-bonds in one dimension to form an H-bond chain. Considering the H-bonds formed in nylon crystals,[70] these H-bonds should exist along the *b* axis because the space between alkyl chains

(70) Tadokoro, H. *Structure of Crystalline Polymers*; John Wiley & Sons: New York, 1979.

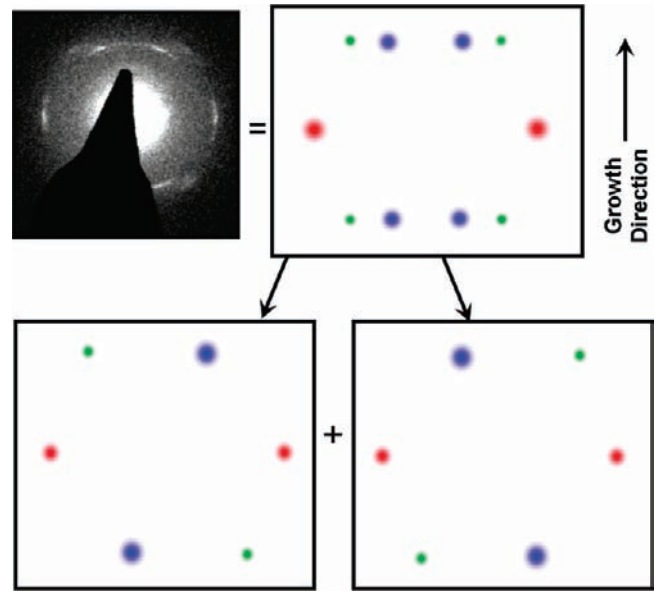

Figure 8. To understand the ED pattern it is divided into two mirror patterns from which the alkyl chain crystal can be determined.

in the *a* axis is too short to contain urethane groups and H-bonds. Figure 10 clearly describes the H-bonds formed between urethane groups in the crystal. In addition, the two amide groups in the PUA block should form H-bond chains in the same manner. Because of the restriction of the dendritic framework, the amide groups in the branch can only form intermolecular H-bonds. And the urethane and amide groups should be positioned in the same direction to form intermolecular H-bonds with the adjacent urethane and amide groups to offer the strongest driving force for one-dimensional growth of the ribbons with a perfect molecular arrangement. These further indicate that the molecular plane of the codendrimer should be normal to the H-bond direction in the ribbon before the alkyl chains crystallize. So the plate-like codendrimer should have janus faces in the ribbon: One face contains N−H groups (the donors of H-bonds) and another face contains C═O groups (the acceptors of H-bonds) mainly because of the difference in bond lengths between N−H (1.012 Å) and C═O (1.208 Å) groups. Such a molecular arrangement avoids any distortions of the molecular framework of the codendrimer, so the urethane and amide groups are in the best position for forming six intermolecular H-bonds and the crystalline packing of the alkyl chains can be optimized. Definitely, the sextuple H-bonds offer the strongest driving forces for codendrimers to grow typically in one dimension into ribbons.

Hierarchical Organization of Codendrimers in Nanoribbon. Self-organization of the codendrimer on the water surface is a hierarchically self-assembling process. The primary ribbon is constructed of a crystalline layer formed by the alkyl chains and the amorphous counterpart of dendritic polyether. According to our previous analysis, we suggest that the plate-like codendrimers in the alkyl chain crystals should arrange as follows: Four adjacent chains along the *a* axis belong to one codendrimer molecule. The plate-like codendrimers stack together along the *b* axis to form a supramolecular ribbon via intermolecular forces. Because of the crystallization of the alkyl chains, the molecular plane and the growth direction of the ribbons now have an angle of 111.5°. Several supramolecular ribbons pack parallel to each other to form a primary ribbon. So, there are six intermolecular H-bonds in the direction of the *b* axis. These strong intermo-

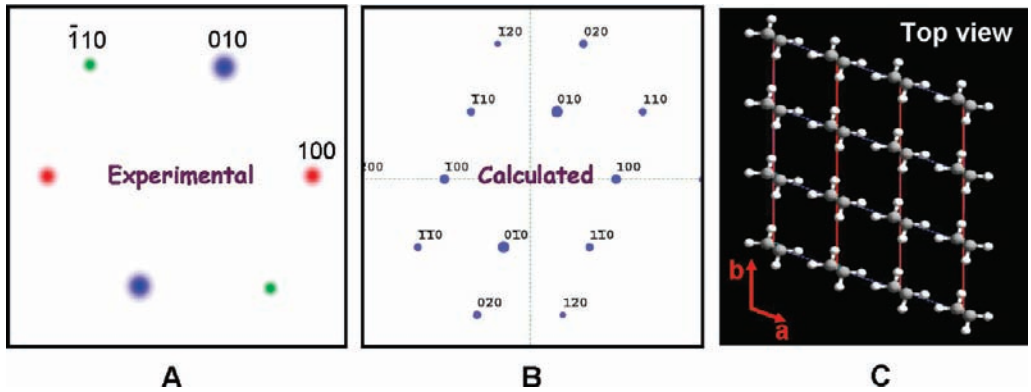

Figure 9. Experimental diffraction pattern, calculated diffraction pattern, and the packing of alkyl chains in crystal units.

Table 1. A Comparison of Calculated Distance and Intensity with Experimental Distance and Intensity

h, *k*, *l*	d_{expt} (Å)	d_{calcd} (Å)	I_{expt}	I_{calcd}
0, 1, 0	4.60	4.61	100%	100%
1, $\bar{0}$, 0	3.90	3.90	47%	49%
1, $\bar{1}$, 0	3.67	3.72	31%	26%

* The unit cell constants of hexadecyl chain crystal are $a = 4.19$ Å, $b = 4.95$ Å, and $c = $ --, $\alpha = 90°$, $\beta = 90°$, and $\gamma = 111.5°$.

lecular interactions direct the codendrimers to pack in the *b* axis direction with the highest growth rate, so the ribbon-like crystals grow micrometers long. Along the *a* axis direction there are only van der Waals interactions between the adjacent codendrimers so that the crystals grow slowly in this direction. That is the reason why the primary ribbon has a short width of *ca.* 7.6 ± 0.5 nm. Here we perform a simple calculation to show that the primary ribbon has a width of five sheets of the codendrimers on average. Since the unit cell constant is $a = 0.419$ nm, the acute angle between the *a* and *b* axes is 68.5°, and five sheets of the codendrimers contain 20 alkyl chains with 19 occupied spaces, we have

$$0.419\ \text{nm} \times \sin 68.5^\circ \times 19 \approx 7.4\ \text{nm}$$

This calculated width is quite close to the 7.6 nm width that was experimentally measured. Figure 11 illustrates the organization of the codendrimers in a primary ribbon. The typical hierarchical organization process follows the following steps: On average the primary ribbons contain five single codendrimer layers of which the width is 1.68 nm. Owing to the plate-like shape of the codendrimer, the primary ribbons seem to be constructed of approximately five supramolecular ribbons. The strong intermolecular H-bonds cause a preferred one-dimensional growth along the *b* axis direction of the alkyl crystals. The secondary ribbons with a 53 ± 6.0 nm width are approximately composed of seven primary ribbons.

Arrangement of the Primary Ribbons in the Secondary Ribbons. So far, we have understood the assembly of the plate-like codendrimer in the primary ribbon through our investigation of the crystal structure of the four alkyl chains on the PUA block periphery. We have stated that there is a 111.5° angle between the molecular plane and the growth direction of the primary ribbon. These results can help us understand the specific electron diffraction pattern obtained in a selected area larger than the width of individual secondary ribbons and then the specific arrangement of the primary ribbons in the secondary ribbons. To facilitate understanding the correlation between structures at different levels and the ED pattern, we prepared a scheme in Figure 12. From the AFM image we can clearly see several primary ribbons embedded in the secondary ribbons. In the figure we schematically show that the ED pattern is captured from an area much larger than a single primary ribbon. The key to understanding the ED pattern is to assume that the molecular planes in adjacent primary ribbons have ±111.5° angles and are mirror-symmetric with respect to the growth direction. In other words, the secondary ribbons consist of the primary ribbons arranged alternatively and in a zigzag manner. Owing to such an arrangement, the final diffraction patterns are a combination of two groups of diffractions contributed by the two kinds of primary ribbons having ±111.5° angles with respect to the growth direction, as shown in the figure as types I and II. In fact the mirror-symmetric arrangements of the type I and II crystals are (100) twins. It is worth noting that simple twins composed of one piece of type I and another piece of type II or a mixture of type I and II single crystals should show similar ED patterns. For the twins or single crystals, they should have faceted ribbon heads. But, our observations, shown in Figures 4A and 6, do not support this argument. In our case the two neighboring primary ribbons are fine, twinned crystals, and their zigzag arrangement results in secondary ribbons.

A Possible Process and Mechanism for Ribbon Formation. It is significant to have a further discussion on the process and mechanism of the hierarchical ribbon formation through a hierarchical assembly of the codendrimer. We believe that the specific structure of the codendrimer is the origin of the hierarchical assembly. So, let us refocus on the chemical structure and functionality of the codendrimer shown in Scheme 1. It is constituted by three functional parts: The first part is the eight hydroxyl groups on the periphery of the PMDC block that provide the hydrophilic function to the individual molecules so they can stand on the water surface to form a monolayer. This is essential to initiating the hierarchical assembly. The second part is the amide and urethane groups in the PUA block that can create multiple H-bonding between molecules so they have janus faces and will recognize each other in a face-to-face manner. This reflects the unique specialty of such plate-like molecules. The last part is the alkyl chains. Their crystallization is the last step in creating the hierarchical assembly. The key point at this step is the formation of a monoclinic lattice. With the statement we will be able to understand the fundamentals of the hierarchical assembly.

Before we go into the details of the process and mechanism, it is worth mentioning that our ED observation shows that the membrane in Figure 1B is amorphous. Based on the morphological and structural analyses of the ribbons, we suggest a possible mechanism to explain the hierarchical assembly to form

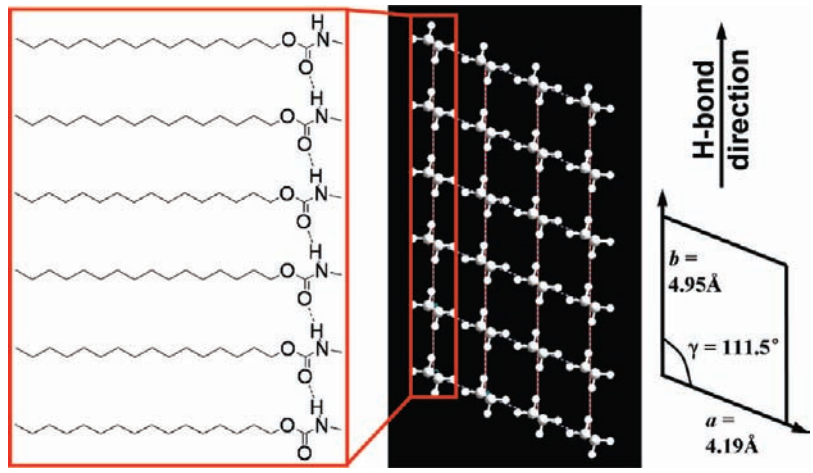

Figure 10. Formation of *trans*-orientational H-bonds between urethane groups in the ribbon-like crystal. Four alkyl chains from the same molecules and the unit cell are presented. The H-bond is directed in the *b* axis.

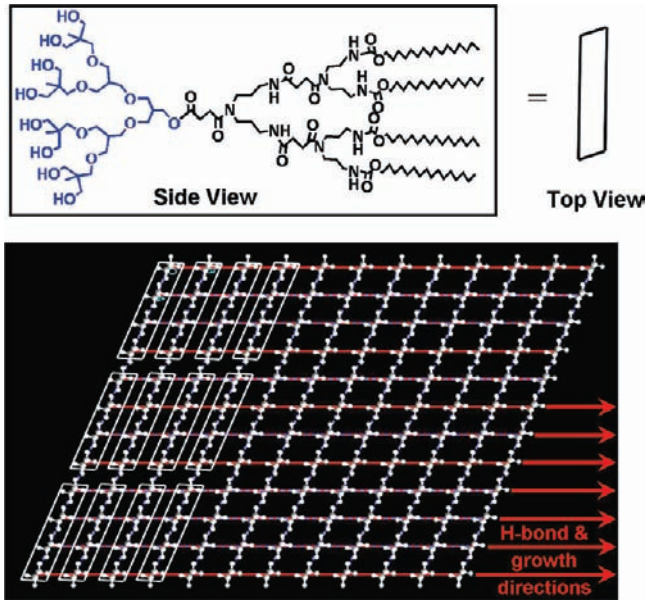

Figure 11. Schematic illustration of molecular organization in a primary ribbon. The H-bond direction is the same as the crystal growth direction. The platelike molecules arrange parallel to each other to form supramolecular ribbons that further constitute the primary ribbon. Note the 111.5° angle between the H-bond (or crystal growth) direction and the molecular plane.

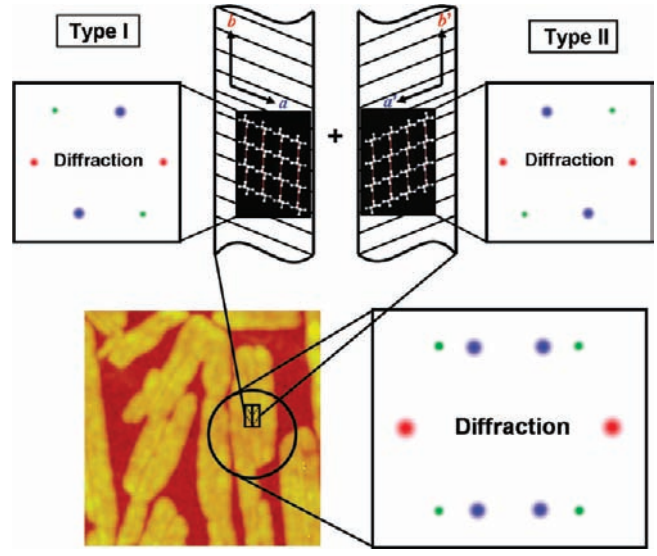

Figure 12. Schematic illustration of the correlation between mirror-symmetrical diffractions and mirror-symmetrically grown primary ribbons. In fact these primary ribbons are twin crystals arranged in a zigzag manner. Their formation originates from the monoclinic lattice of the alkyl chain crystal.

the ribbons through a multiple-step ordering process of the codendrimer. Figure 13 schematically presents the process of molecular recognition, assembly, and crystallization of the codendrimer. When a certain amount of codendrimers was spread onto the water surface to form a domain, the molecules stand at the interface randomly in the domain at the beginning. On the molecular scale, the following step is a molecular recognition directed by the multiple intermolecular H-bonds between the codendrimers. In consideration of the features of the plate-like shape and janus faces of the codendrimer, the recognition step is very important for further stacking into an ordered arrangement. The donor face of the multiple H-bonds of one codendrimer can exactly form multiple H-bonds with the corresponding acceptor face of multiple H-bonds of the neighboring molecule. Therefore, the recognition of these H-bonds guides the codendrimers into a face-to-face packing to form supramolecular arrangements. The final step is a ribbon-like self-organization accompanied with cooperative crystallization of four alkyl chains belonging to the same codendrimer. Clearly, the crystallization rate can be promoted and the degree of crystallization can be maximized by the formation of ordered arrangements of the codendrimers guided by the multiple H-bondings.

In Figure 14 we suggest a possible process for ribbon formation on the micrometer scale. At the beginning the codendrimers immediately aggregate into pieces of liquid-like monolayer membranes (see Figure 14A). Because of the molecular recognition mechanism, a rapid crystal nucleation−growth occurred at a part of the membrane (see Figure 14B). Considering the character of the alkyl chain crystal growth with a unit cell of the monoclinic lattice and the plate-like shape of the codendrimer, it is reasonable to suggest that the *anisotropic* crystal growth originates from the ribbon-like crystal formation in the liquid-like domains. In crystallography it is very common that anisotropic crystal growth will produce a needle-like crystal because an active plane has a higher surface free energy, so crystals grow faster in the direction perpendicular to the plane.

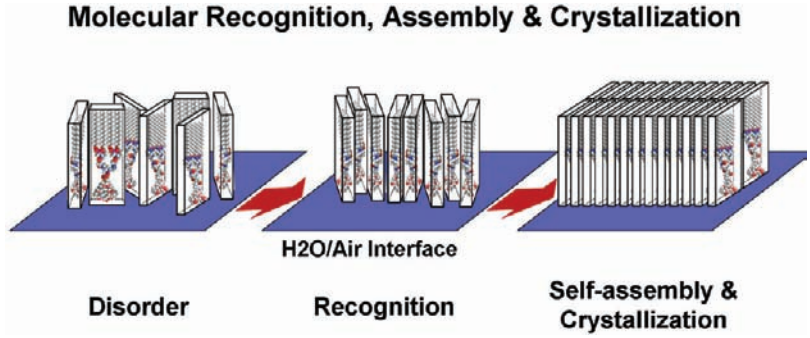

Figure 13. Schematic representation of the platelike molecular recognition, assembly and crystallization within the single molecular layer on the water surface.

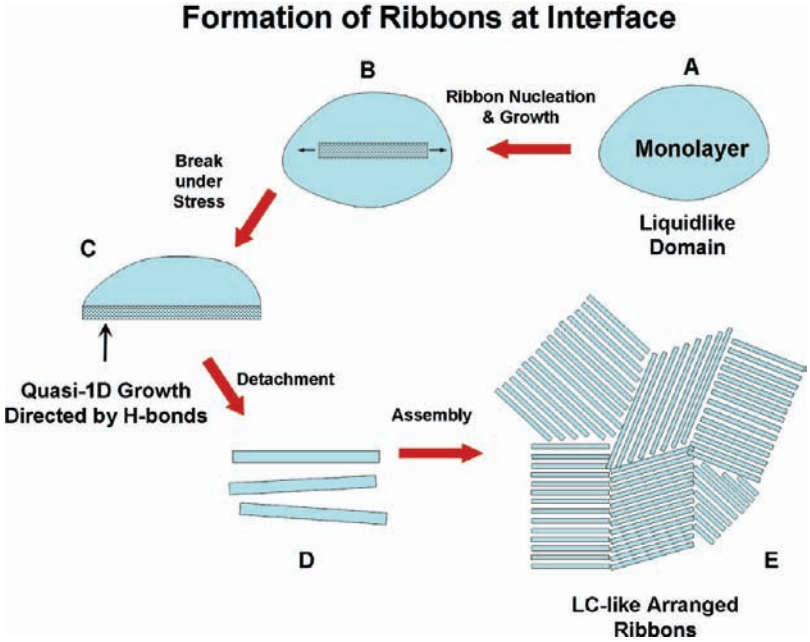

Figure 14. Suggested processes of the formation of the ribbons at the interface.

Since there is a 111.5° angle between the crystal growth direction and the molecular plane, the four alkyl chains in the same codendrimer will be able to crystallize in planes having a plus or minus 111.5° angle with regard to the growth direction, that is, a twinnig mechanism. This selective growth results in the formation of the crystal ribbons that contain a couple of zigzag-arranged fine ribbon-like twin crystals, rather than large single crystals. The ribbon crystal grows in the two directions until it reaches the edge of the membrane. So, the domains consist of the crystalline and ordered ribbon(s) coexisting with some disordered membranes (or the flags). Because of the different mechanics there exists a strain between the membrane and ribbon-like crystals, so a crack can grow along the interface between ribbons and membranes to part each other, as schematically presented in Figure 14C. This is the reason for forming the flag-like membranes (see Figure 1B). Once the ribbons have detached themselves from the disorder membranes, they float on the water surface and can form an ordered pattern at the water−air interface when they are pressured by a lateral force (see Figure 14D). The pattern in Figure 2 or 6 is the same as those formed by rodlike molecules in their liquid crystal phase. Significantly, the supramolecular and straight ribbons are the elements of constructing the patterns with liquid crystal order. Such a process will result in a size decrease but a number increase of the disorder membrane domains, so the short ribbons are more popular than the long ones. This is the point that is shown in Figure 3B.

Conclusions

In summary we have studied the hierarchically self-assembled structure of the amphiphilic and plate-like codendrimer with a janus face on the water surface. Different from the traditional surfactants or amphiphilic copolymers, the eight hydroxyl groups are on one side of the codendrimer and the four alkyl groups are on another side, and the two amide and four urethane groups are in the body of the codendrimer that can provide sextuple H-bonding between molecules. In our investigation on the self-assembled structure, we found that such a specific molecular structure produces a plate-like shape of which one face has six N−H groups and another face has six C═O groups. So, the assembly of the codendrimer started through molecular recognition: The N−H face of a molecule recognizes the C═O face of another molecule to generate a full match of the six H-bond sites. This will further produce the maximum driving force for the molecules in facilitating their assembly into a 1D supramolecular object in which the crystallization of the alkyl chains can be maximized. Because of the monoclinic lattice, there is a 111.5° angle between the crystal growth direction and the

molecular plane. This is the origin of a primary ribbon with a twin feature forming in the secondary ribbon through a zigzag manner. Our investigations have clearly shown that the existence of the hierarchical structure at the different scales comes from the hierarchical self-assembly processes of the codendrimer, which is closely associated with its janus and plate-like features, multiple H-bonding, and the crystallization of alkyl chains. Obviously, the molecular self-assembly of the codendrimer in the monolayer has several features in process and mechanism different from those of conventional surfactants or amphiphilic copolymers. The results reported in this work provide a new strategy in designing and creating novel nanomaterials with well-defined structures at different scales.

Acknowledgment. This work was supported by the National Science Foundation of China (NSFC Grant Nos. 20374030 and 20734001). Yang thanks the International Max-Planck Research School for support his stay in Germany.

Supporting Information Available: Experimental details, ^{1}H and ^{13}C NMR, MALDI-TOF, MS, infrared spectra. This material is available free of charge via the Internet at http://pubs.acs.org.

JA900739E